Review Article

Ion-specific effects on equilibrium adsorption layers of ionic surfactants

Stoyan I. Karakashev

Department of Physical Chemistry, Sofia University, Sofia 1164, Bulgaria. E-mail: fhsk@chem.uni-sofia.bg

ABSTRACT

This review article reports the effect of the counter-ions on the ionic surfactant adsorption layer and its relation to the stability of foams and emulsions. The adsorption theory of Davies about the ionic surfactant monolayer was revisited and it is shown how to account for the type of the counter-ions. The experimental validation of this theory on thin liquid films was shown as well, thus explaining the effect of Hofmeister. However, their effect on foams and emulsions is more complex. Furthermore, it is shown how the counter-ions affect in complex way the stability of foams and emulsions via the surfactant adsorption layer in the light of the newest theory. To elucidate the nature of this effect, further investigation is called for.

Keywords: Ionic Surfactants; Ion Specific Effects; Effect of Hofmeister

1. Introduction

Hofmeister was the first to report how the solubility of the proteins depends on the added salt[1-7]. Hence, he established that some salts are stronger precipitators than other ones. He found out that both cations and anions act together but the effect of the anions is stronger. Thus, the anions and cations were ordered according to their precipitation ability:

Cations: $Li^+ < Na^+ < NH_4^+ < K^+ < Cs^+$

Anions: $OH^- < F^- < CH_3COO^- < Cl^- < Br^- < NO_3^- < I^- < ClO_4^-$

The ion sequence in the above series is independent of the protein, but their precipitation strength depends on the sign of the protein's net charge as well. Since that time, it was established that the salts precipitate in the same manner surfactants, colloidal particles and other more complex systems[8]. Evidently, the difference between the ionic parameters (size, polarizability, and ionization potential)[9] make them act differently on proteins, surfactants, colloidal particles, etc. A more detailed analysis on the effect of Hofmeister reveals that the ions adsorb on the surfaces of the colloids on different levels, thus affecting differently the interaction between the colloids (protein molecules, solid particles, surfactants, bubbles, oil droplet, etc.). For example, Ninham *et al.*[10-12] accounted for the van der Waals in teraction between inorganic ions and the bubble, thus determing concentration profiles of the different ions, but further met difficulties[13-15]. Tavares *et al.*[16] studied theoretically the Hofmeister effect on the interaction of charged proteins and established that van der Waals interaction causes strong attraction between the molecules. Warszynski *et al.*[17-19] and

Aratono et al.[20-22] clearly showed experimentally the specific effect of the counter-ions on the state of the adsorption layer of ionic surfactants, but Davies[23,24] and Borwankar and Wasan[25] showed the way for their theoretical interpretation. Later on Ivanov et al.[26-28], combined the approaches of Ninham[10-12] and Davies[23,24] to produce a relatively simple theory on the specific adsorption of counter-ions within adsorption layer of ionic surfactant. This theory accounts for KCl major factors controlling the ion specific adsorption: the ion polarizability and ionization potential, the radius of the hydrated ion and the possible deformation of the hydration shell upon ion adsorption at the interface. Ref.[29] successfully applied this theory to model disjoining pressure of thin liquid films, and emulsion stability between the film surface. We will present here after the basis of this theory along with its attempt to predict the foam and emulsion stability.

2. Ion-specific effects on the adsorption layers of ionic surfactants from dilute solutions

2.1. Adsorption in the absence of ion specific effects

It is well-known that adsorption Γ_{0s} of nonionic surfactant with concentration C_s in scarce adsorption layer is described by Henry adsorption isotherm:

$$\Gamma_{0s} = K_s C_s \tag{1}$$

Accordingly, the Henry equation of state is as following:

$$\sigma = \sigma_0 - RT\Gamma_{0s} \tag{2}$$

Where, σ and σ_0 are the surface tensions of the surfactant solution and the solvent, R and T are the gas constant and temperature.

If we assume that the adsorption layer becomes ionized equation (1) gets the form:

$$\Gamma_{0s} = K_s C_s exp\left(-\frac{F\Psi_{0s}}{RT}\right) \tag{3}$$

Where, F and ψ_{0s} are the Farady constant and the surface potential of the adsorption layer with excluded counter-ions.

Next, we regard the Poisson-Boltzmann equation in rectangular reference of state along the axis z:

$$\varepsilon\varepsilon_0\frac{d^2\Psi_{0s}}{dz^2} = -\sum_i z_i F C_{0i} exp\left(\frac{-z_i F\Psi}{RT}\right) \tag{4}$$

Where, z_i is valency of the ion of species i, and ε and ε_0 are dielectric permitivities of the aqueous medium and the free space, while C_{0i} is the electrolyte concentration of type i.

In this equation, the variables Ψ and $d\Psi/dz = -E$ (electric field) can be separated, by using the identity $2d^2\Psi/dz^2 = d(E^2)/d\Psi$. This leads to:

$$d(E^2) = -\frac{2}{\varepsilon\varepsilon_0}\sum_i F z_i C_{0i} exp\left(\frac{-z_i F\Psi}{RT}\right)d\Psi \tag{5}$$

A first integral of the Poisson-Boltzmann equation is obtained by integrating equation (5) in limits $z = \infty$ to z, using as a first boundary condition $E = 0$ and $\Psi = 0$ at $z = \infty$:

$$E(z^2) = \frac{2RT}{\varepsilon\varepsilon_0}\sum_i C_{0i}\left[exp\left(\frac{-z_i F\Psi}{RT}\right) - 1\right] \tag{6}$$

The second boundary condition (at $z = 0$) is the electro neutrality condition:

$$\varepsilon\varepsilon_0 E|_{s=0} = F\Gamma_{0s} \tag{7}$$

We will denote the surface potential $\Psi(0)$ by Ψ_{0s}. Setting $z = 0$, Ψ and Ψ_{0s} into equation (6), and eliminating $E(z = 0)$ from the electroneutrality condition (7), the Gouy equation is obtained:

$$\frac{k_0^2}{4}\Gamma_{0s}^2 = \sum_i C_{0i}\left[exp\left(\frac{-z_i F\Psi_{0s}}{RT} - 1\right)\right] \tag{8}$$

Here,

$$k_0^2 \equiv \frac{2F^2}{\varepsilon\varepsilon_0 RT} \tag{9}$$

Equation (9) is the concentration independent part of Debye parameter: $k^2 = k_0^2 C_t$. In the case of 1:1 electrolyte, Gouy's equation (7) simplifies to:

$$\frac{k_0}{4}\Gamma_{0s} = \sqrt{C_t}sinh\left(\frac{\Phi_{0s}}{2}\right) \tag{10}$$

Here, C_t is the total electrolyte concentration (in units [m^{-3}]) and

$$\Phi_{0s} = \frac{F\Psi_{0s}}{RT} \tag{11}$$

is the dimensionless positively defined surface potential. At high surface potentials ($\Phi_s >> 1$), a good approximation of Gouy equation (10) is:

$$\Gamma_{0s} = \frac{2}{k_0}\sqrt{C_t}exp\left(\frac{\Phi_{0s}}{2}\right) \tag{12}$$

The ion distribution in the electrical double layer depends on the local potential $\Phi(z)$. Hence, the ion adsorption Γ_i^{DL} of any ion i in the diffuse layer can be calculated by using Gibbs definition of adsorption as an excess:

$$\Gamma_i^{DL} \equiv C_{0i}\int_0^\infty [exp(-z_i\Phi(z)) - 1]dz \tag{13}$$

Where, the superscript "DL" indicates counter-ions, co-ions and surfactant ions in the diffuse layer only. Generally, the total surfactant adsorption

is a sum of Γ_i^{DL} and the surface concentration Γ_s (adsorption in the adsorption layer). The surfactant ions in the diffuse layer are repelled by the interface since they have the same charge and the surface potential Φ_s is enough high. Hence, the surfactant concentration in the diffuse layer tends to zero and can be neglected. The same refers to the co-ions. Therefore, only the adsorption of the counter-ions in the diffuse layer is important. In order to calculate the integrals defined by equation (13), it is convenient to change the integration variable to Φ, by using the relation $dz = d\Phi/(d\Phi/dz)$, and neglecting the co-ions in DL, equation (13) can be reduced to:

$$\Gamma_i^{DL} \equiv C_{0i} \int_{\Phi_s}^{0} \frac{[exp(\Phi(z))-1]}{d\Phi/dz} d\Phi \qquad (14)$$

By using Poisson-Boltzmann equation (4) to obtain expression for $d\Phi/dz$:

$$\frac{d\Phi(z)}{dz} = -k_0\sqrt{C_t}[exp(\Phi(z)) - exp(-\Phi(z))] \qquad (15)$$

One can obtain explicit expression for the adsorptions Γ_i^{DL}:

$$\Gamma_i^{DL} = \frac{2C_{0i}}{k_0\sqrt{C_t}}\left[exp\left(\frac{\Phi_{0s}}{2}\right) - 1\right] \xrightarrow{\Phi_{0s}\to\infty} \frac{2C_{0i}}{k_0\sqrt{C_t}}exp\left(\frac{\Phi_{0s}}{2}\right) \qquad (16)$$

To calculate the surface tension, the Gibbs isotherm is used. If only one counterion of concentration C_{0i} is present in the system, and the bulk solution is assumed ideal, one has:

$$d\sigma = -RT\Gamma_s dlnC_s - RT\Gamma_i^{DL} dlnC_{0i} \qquad (17)$$

For high surface potential, one has $\Gamma_i^{DL} = \Gamma_s$. Then, the Gibbs isotherm (17) simplifies to:

$$d\sigma = -2RT\Gamma_s dlnC \qquad (18)$$

Where, C is the mean ionic activity of the surfactant[30,31], defined by:

$$C = C_s^{1/2} C_i^{1/2} \qquad (19)$$

If the solution is not ideal, the mean ionic activity C in equation (19) will include activity coefficient:

$$C = \gamma C_s^{1/2} C_i^{1/2} \qquad (20)$$

Meanwhile, the combination of equations (3) (Henry adsorption isotherm for ionic surfactants) and (12) (Gouy equation) produce the following important relation[23,28]:

$$3\Phi_{0s} = ln\frac{\kappa_0^2 K_s^2}{4} + ln\frac{C_s^2}{C_t} = 6ln\frac{\kappa_0 K_0}{2} + ln\frac{C_s^2}{C_t} \qquad (21)$$

Equation (21) shows that the surface potential Φ_s increases with C_s and K_s (due to the increased adsorption) and decreases with the total electrolyte concentration C_t (due to the additional screening effect of the electrolyte on the surface charge). Inserting back, the surface potential (21) into the isotherm (3), one obtains a generalization of Henry isotherm for adsorption of ionic surfactants:

$$\Gamma_{0s} = K_0 C^{2/3} \qquad (22)$$

Where, C is given by equation (19), and K_0 is adsorption constant of the ionic surfactant. It is related to Henry constant K_s:

$$K_0 = (4K_s/\kappa_0^2)^{1/3} \qquad (23)$$

The fact is that, according to equation (22), Γ_s depends only on the mean ionic activity. C is an explicit formulation of what is known as salting out effect on ionic surfactant adsorption[31]. Equation (22) has been first derived and confirmed by experimental data for $C_nH_{2n+1}SO_4Na$ at air/water interface by Davies[23]. We will refer to it as Davies isotherm. By using the procedure of Borwankar and Wasan[25], and Ivanov *et al.* derived equation (22) and obtained the explicit expression (23) for K_0. According to equation (23), K_0 should not depend on the electrolyte concentration, at least for moderate concentrations. Substituting equation (22) in the Gibbs isotherm (18) and integrating, one obtains Davies equation of state[32]:

$$\sigma = \sigma_0 - 3RTK_0 C^{2/3} \qquad (24)$$

Equation (24) does not account for the specific effect of the counter-ions. Hence, according to this equation, if the counter-ion of one ionic surfactant is replaced by another counter-ion, its surface activity will not change. The latter controversies to the experimental data[33]. For this reason, the real equilibrium adsorption constant K, in which the specific adsorption of counter-ions is accounted for, has been modelled[26] by the following relation:

$$K = K_0 exp\left(-\frac{u_0}{2k_B T}\right) \qquad (25)$$

Where, k_B is the Boltzmann constant, and u_0 is the specific adsorption energy of the surfactant's counter-ion.

2.2. Adsorption in the presence of ion-specific effects

To account for the specific adsorption of the counter-ions into the surfactant adsorption layer, one should account for the correction, which they cause to the electric potential in the Poisson-Boltzmann equation:

$$\varepsilon\varepsilon_0\frac{d^2\Phi}{dz^2} = -\sum_i z_i FC_{0i} exp\left[-z_i\Phi(z)-\left(\frac{u_i(z)}{k_BT}\right)\right] \quad (26)$$

Where, $u_i(z)$ is the specific interaction between the ion and the interface[26,28] given by the relation:

$$u_i(z) = \frac{R_i^3}{(R_i+z)^3}u_{i0}. \quad (27)$$

Here, R_i is the ionic radius and u_{i0} is the van der Waals energy of an ion in the plane $z = 0$ situated at distance R_i from the interface as shown in **Figure 1**. This equation can be integrated by analogy with the derivation of Gouy equation (10), by using $2d^2\Phi/dz^2 = d(E^2)/d\Phi$ and Gauss condition (7):

$$F^2\Gamma_{0s}^2 = -2\varepsilon\varepsilon_0\sum_i z_i FC_{0i}exp\left(-\frac{u_{i0}}{k_BT}\right)$$
$$\int_0^{\Phi_{0s}} exp[-z_i\Phi(z)]exp\left[-\frac{u_i(z)-u_{i0}}{k_BT}\right]d\Phi \quad (28)$$
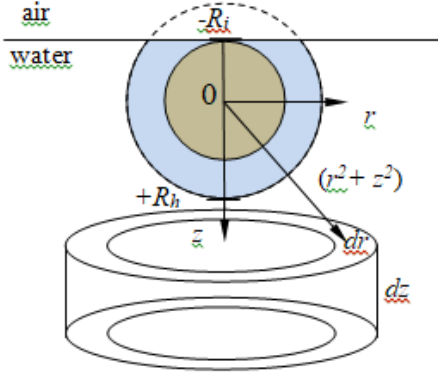

Figure 1. Illustration of the integration procedure applied to derive the energy of interaction of surface ion with the whole bulk of water[26].

At high surface potentials, only the counterions need to be taken into account in the sum in the right-hand side of this equation. This approximation is of crucial importance for this theory to simplify all following calculations. It can be used also in the case of ionized proteins and polymers as well, but not for the adsorption of simple electrolytes. In such a case, both cations and anions have comparable participation in the diffuse layer, whose local potential depends, in fact, on the small difference of their local concentrations. With this approximation, the integrals in the right hand side of equation (28) can be reduced to a generalized Gouy equation, accounting for the ion specific effect:

$$\Gamma_{0s}^2 = \frac{4}{k_0^2}\sum_i C_{0i}exp\left(-\frac{u_{i0}}{k_BT}\right)exp(\Phi_{0S}) \quad (29)$$

Where, k_0 is the Debye parameter which is given by equation (9), and Φ_{0s} is surface potential of adsorption layer situated on the phase boundary, not containing counter-ions. If only one counter-ion is present in the system, equation (29) simplifies to:

$$\Gamma_{0s}^2 = \frac{4}{k_0^2}C_t exp\left(-\frac{u_{i0}}{k_BT}\right)exp(\Phi_{0S}) \quad (30)$$

Substituting here, the expression for Φ_{0s}, equation (23), one obtains expression of Davies adsorption isotherm (22), $\Gamma_{s0} = K_0 C^{2/3}$, accounting for ion specific interactions:

$$\Gamma_{0s} = K_0 exp\left(-\frac{u_{i0}}{2k_BT}\right)C^{2/3} \equiv KC^{2/3} \quad (31)$$

Here, C is the mean activity. Therefore, one can obtain the following expression for the equilibrium adsorption constant accounting for the ion-specific effects:

$$K = K_0 exp\left(-\frac{u_{i0}}{2k_BT}\right) = \left(\frac{4K_s}{k_0^2}\right)^{1/3}exp\left(-\frac{u_{i0}}{2k_BT}\right) \quad (32)$$

This procedure allows also the determination of the first iteration for the real surface potential Φ_s. To do so, the equation of state (3) is used, with Γ_s given by equation (31). After solving the result with respect to Φ_s, one obtains:

$$\Phi_s = \frac{1}{3}ln\frac{k_0^2 K_s^2}{4} - \frac{1}{3}ln\frac{C_s^2}{C_t} + \frac{u_{i0}}{2k_BT} \quad (33)$$

Considering the above equations, one can obtain the following relations:

$$\Gamma_s = \Gamma_{0s}exp\left(-\frac{u_{i0}}{2k_BT}\right), \quad \Phi_s = \Phi_{0s}+\frac{u_{i0}}{2k_BT} \quad (34)$$

Where, Γ_s and Γ_{0s} are surfactant adsorption containing and not containing counter-ions, and Φ_s and Φ_{0s} dimensionless surface potentials containing and not containing correction from the adsorption of counter-ions. Hence, equation (24) gets the form:

$$\sigma = \sigma_0 - 3RTKC^{2/3} \quad (35)$$

Equation (35) is valid for liquid expanded state of the adsorption layer, which is medium term level of occupation of the latter. Moreover, the constant σ_0 is not anymore the surface tension of the solvent (water), but cohesion constant.

The next step is modelling the specific adsorption energy u_{i0} of the counter-ions onto the air/water interface.

2.3 Theory on adsorption of ions on the air/water interface

The adsorption of inorganic ion on the air/water interface may seem inappropriate at first glance due to the image repulsion[34], but one should account for the displaced surface water molecules by the adsorbed inorganic ion. The latter can make this adsorption energetically favorable. For this reason, the effect of Ray-Jones[35] appears at
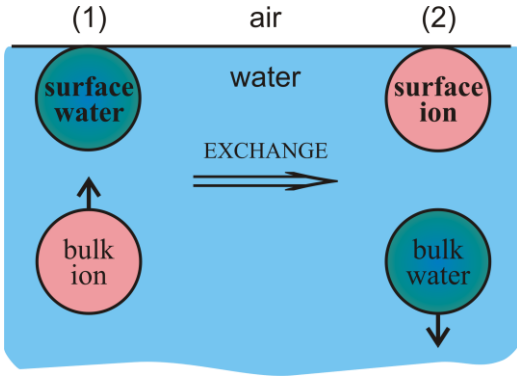
small salt concentrations (up to 0.1 M).

Figure 2. Energetical states prior and after the adsorption of ion on air/water interface.

We assume that one ion displaces N_w water molecules from the air/water interface, and the latter dive into the bulk. Shown in **Figure 2** are the energetical states 1 and 2 of the adsorption of inorganic ion on the air/water interface. Energetical state 1 consists of inorganic ion in the bulk and N_w water molecules at the air/water interface. Both of them interact with the whole bulk of water molecules. Energetical state 2 consists of inorganic ion at the air/water interface and the displaced N_w water molecules being already into the bulk. Again both of them interact with the whole bulk of water molecules. The energy of the very process is the difference between the energies of the two states:

$$u_0 = \left(u_{iw}^s + u_{ww}^b\right) - \left(u_{iw}^b + u_{ww}^s\right) = \Delta u_i - \Delta u_w \quad (36)$$

Where, u_{iw}^s is the energy of interaction of the surface ion with the whole bulk of water, u_{ww}^b is the energy of interaction of N_w water molecules located in the bulk with the whole bulk of water molecules, u_{iw}^b is the energy of interaction of one inorganic ion located in the bulk with the whole bulk of water, u_{ww}^s is the energy of interaction of N_w water molecules located on the air/water interface with the whole bulk of water, Δu_i is the difference between energetical states of ion on the surface referred to the bulk, and finally Δu_i is the difference of the energetical states of N_w water molecules on the surface referred to the bulk. To calculate the specific energy of adsorption u_0 of one ion on the air/water interface, one needs to calculate each of the above mentioned quantities[26,28]. Moreover, a special accent[26,30] is put on the compressibility of the hydration shells – there are certain ions,

called kosmotrops[36.37] (or structure making, e.g. Li^+, Na^+, F^-), whose hydration shell does not deform upon their adsorption on the air/water interface, while the hydration shells of all the other ions called chaotrops[36,37] (or structure breaking, e.g. K^+, Cl^-, Br^-, NO_3^-, etc.), redistribute in such a way during their adsorption on the air/water interface that the upper part (toward air) of the ion becomes bare, while the lower part (toward the bulk) becomes over-occupied with hydrated water molecules (see **Figure 3**). The calculation of the energy u_{i0} was performed, using the London expression for the intermolecular potential u_{ij} between molecules of type i and j at a distance r_{ij}[34]:

$$u_{ij} = -L_{ij}/r_{ij}^6 \quad (37)$$

Where, the London constant L_{ij} is related to the static polarizabilities $\alpha_{p,i}$ and $\alpha_{p,j}$ and the ionization potentials I_i and I_j of the interacting species:

$$L_{ij} = \frac{3\alpha_{p,i}\alpha_{p,j}}{2} \frac{I_i I_j}{I_i + I_j} \quad (38)$$
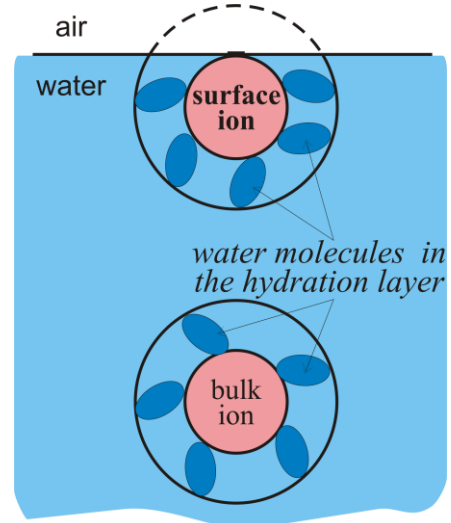

Figure 3. Redistribution of the hydration shell during the adsorption of ion on the air/water interface. Reprinted with permission from ref.[26]. Copyright 2007 Elsevier.

We will calculate first the energy of interaction u_i^s of the chaotropic type of ions situated on the air/water interface with the whole bulk of water. Toward this aim, the London potential (36) is integrated over the volume of the water phase excluding the hydration shell, with r_{ij} being the distance between the volume element dr and the ion positioned at $r = 0$, $z = 0$ (that is, the integration is over $z > -R_b$ and $r^2 + z^2 < R_h^2$). The integration is performed in cylindrical coordinates (see **Figure 1**):

$$u_i^S = -\int_{-R_b}^{R_h} \int_{\sqrt{R_h^2-z^2}}^{\infty} \frac{L_{iw}\rho_w 2\pi r dr dz}{(r^2+z^2)^3}$$

$$-\int_{R_h}^{\infty} \int_0^{\infty} \frac{L_{iw}\rho_w 2\pi r dr dz}{(r^2+z^2)^3} = -\frac{2\pi}{3}\frac{L_{iw}\rho_w}{R_h^3}\left(1+\frac{3}{4}\frac{R_b}{R_h}\right) \quad (39)$$

Here, ρ_w is the particle density of water. Similarly, the energy u_i^B of interaction of ion located in the bulk with the whole bulk of water (integration in spherical coordinates):

$$u_i^B = -\int_{R_h}^{\infty} \frac{L_{iw}}{r_w^6}\rho_w 4\pi r_{iw}^2 dr_{iw} = -\frac{4\pi}{3}\frac{L_{iw}\rho_w}{R_h^3} \quad (40)$$

The respective energies of the ensemble of water molecules (assumed a sphere of radius R_h, or a part of it) are:

$$u_w^S = -\frac{2\pi}{3}\frac{L_{ww}\rho_w}{R_h^3}\left(1+\frac{3}{4}\frac{R_b}{R_h}\right)$$

$$u_w^B = -\frac{4\pi}{3}\frac{L_{ww}\rho_w}{R_h^3} \quad (41)$$

Substituting equations (39)-(41) into the expression (34) for u_{i0}, one obtains an explicit relation of the adsorption energy of the chaotropic ions (called here ions of type I):

$$u_{i0} = \left(1-\frac{3}{4}\frac{R_b}{R_h}\right)\frac{2\pi}{3}\frac{\rho_w}{R_h^3}(L_{iw}-L_{ww}) \quad (42)$$

To calculate u_{i0} for the kosmotrops (called here ions of type II), one must set $R_h = R_b$ in equation, which simplifies the expression to：

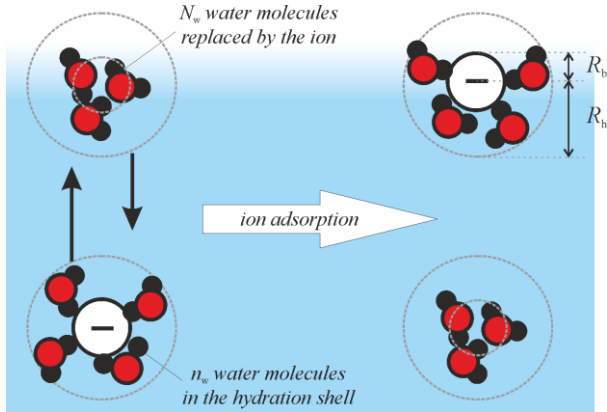$$u_{i0} = \frac{\pi}{6}\frac{\rho_w}{R_h^3}(L_{iw}-L_{ww}) \quad (43)$$

Figure 4. Scheme of the process of adsorption of a type I ion. Left: ion in the bulk. Right: ion at the surface. The n_w hydrating water molecules might be pushed away by the interface, so that the shortest distance of approach of the ion to the interface is the bare ion radius R_b. Upon adsorption, the ion replaces an ensemble of N_w water molecules. For type II ions, the shortest distance of approach of the ion to the interface is the hydrated ion radius R_h.

For monovalent ions, Marcus[38] found that the hydration number n_w of the ions can be represented by the empirical relation:

$$n_w = A_v/R_i \quad (44)$$

Where, $A_v = 3.6$ Å for all ions. He further as-sumed that the hydrating n_w water molecules, considered as spheres with radius $R_w = 1.38$ Å and volume $v_w = 11$ Å^3, are squeezed around the ion, forming a layer of thickness $R_h - R_b$ and volume:

$$n_w v_w = \frac{4\pi}{3}\left(R_h^3-R_b^3\right) \quad (45)$$

The last relation can be used to calculate R_h. The values of n_w and R_h calculated in this way[26,38,39] are shown in **Table 1**. Robinson and Stokes[30] used similar approach, but with water molecular volume $v_w = 30$ Å^3, which follows from the density of water. They also used different values of the hydration number n_w, which were calculated from the ion diffusivity.

The London constants L_{iw} for the interaction ion-water molecule, and L_{ww} for the interaction of N_w water molecules with a single water molecule are calculated directly from equation:

$$L_{iw} = \frac{3\alpha_{p,i}\alpha_{p,j}}{2}\frac{I_iI_w}{I_i+I_w}$$

$$L_{ww} = \frac{3}{4}N_w\alpha_{p,w}^2 I_w \quad (46)$$

For the calculation of L_{ww}, the ensemble of N_w water molecules is regarded as a sphere with polarizability $N_w\alpha_{p,w}$[26]. The number N_w was assumed equal to the ratio between the volume of the bare ion and the volume of one water molecule[40]:

$$N_w = R_b^3/R_w^3 \quad (47)$$

Where, R_w is the radius of the water molecule. For the value of R_w, two possibilities were tested in Ref.[26]: (i) the average volume per molecule (30 Å^3), based on the water density, yields $R_w = 1.93$ Å; and (ii) the proper volume of a water molecule, 11 Å^3, corresponds to $R_w = 1.38$ Å. Better agreement with the experimental data was obtained with the second option, $R_w = 1.38$ Å. The used value of the static polarizability of water was $\alpha_{p,w} = 1.48$ Å^3 and of the ionization potential was $I_w = 2.02\times10^{-18}$ J[41].

For the cations, we used the second ionization potential, since the first one corresponds to ionization of the respective atom, not ion. Since the anions have already accepted one extra electron, their ionization potential must be equal to the negative value of the electron affinity.

Table 1. Specific adsorption energies of the considered ions (T = 25°C)

cation	R_b [Å]	n_w Eq. (66)	R_h [Å] Eq. (67)	N_w Eq. (69)	L_{ww} Eq. (68) [m^{6}J] ×10^{80}	$\alpha_{p,i}$ [Å^3]	I_i [J] ×10^{18}	L_{wi} Eq. (68) [m^{6}J] ×10^{80}	u_{i0}/k_BT type I Eq. (64)	u_{i0}/k_BT type II Eq. (65)
Li$^+$	0.69[1]	5.22	2.41	0.13	41.5	0.03[1]	12.1[2]	11.5		–0.09
Na$^+$	1.02[1]	3.53	2.18	0.40	134	0.15[3]	7.58[2]	53.1		–0.33
NH$_4^+$	1.53[4]	2.35	2.14	1.36	453	1.64[1]	2.13[2]	378	–0.61	
K$^+$	1.41[1]	2.55	2.12	1.07	354	0.79[3]	5.07[2]	253	–0.90	
Rb$^+$	1.65[5]	2.18	2.17	1.71	568	1.4[1]	4.41[2]	431	–0.98	
NMe$_4^+$	2.80[1]	1.29	2.94	8.36	2770	9.08[1]	2.43[2]	2220	–1.05	

anion	R_b [Å]	n_w	R_h [Å]	N_w	L_{ww} [m^{6}J] ×10^{80}	$\alpha_{p,i}$ [Å^3]	I_i [J] ×10^{18}	L_{wi} Eq. (68) [m^{6}J] ×10^{80}	u_{i0}/k_BT type I	u_{i0}/k_BT type II
Ac$^-$	1.65[1]	2.18	2.17	1.71	568	5.50[1]	0.544[1]	545		–0.185
OH$^-$	1.33[1]	2.71	2.11	0.90	297	2.04[1]	0.345[1]	134		–0.736
F$^-$	1.33[1]	2.71	2.11	0.90	297	1.04[2]	0.545[1]	99.1		–0.891
Cl$^-$	1.64[1]	2.20	2.17	1.68	557	3.59[2]	0.580[1]	359	–1.43	
Br$^-$	1.95[1]	1.85	2.31	2.82	937	5.07[2]	0.540[1]	480	–2.32	
NO$_3^-$	2.00[1]	1.80	2.33	3.05	1010	3.93[1]	0.631[1]	420	–2.83	
N$_3^-$	1.95[1]	1.85	2.31	2.82	937	4.45[1]	0.444[1]	360	–2.93	
ClO$_4^-$	2.40[1]	1.50	2.61	5.26	1750	5.25[2]	0.758[1]	642	–3.28	
BF$_4^-$	2.30[1]	1.57	2.53	4.63	1540	2.80[1]	0.902[1]	388	–3.84	

Note: R_b – bare ion radius; n_w – hydration number, Eq. (44); R_h – hydrated ion radius, Eq. (45); N_w – number of water molecules in the ensemble, replaced by the ion upon adsorption, Eq. (47); L_{ww} – London constant of this ensemble, Eq. (46); $\alpha_{p,i}$ – polarizability of the ion; I_i – second ionization potential of the cations and negative electron affinity of the anions; u_{i0} – ion specific adsorption energy, Eq. (42) for type I ions (no deformation of the hydration shell) and Eq. (43) for type II ions (with deformation of the hydration shell). The ions in the Table are ordered by increasing absolute values of u_{i0}. The sequence of both cations and anions is the same as in Hofmeister series, but for the cations this order corresponds to increasing efficiency as opposite to the series. Source data: [1]Marcus[38]; [2]Nikolskij[41]; [3]Tavares[16]; [4]Dietrich[42]; [5]Lide[43]

3. Comparison with experiment

3.1. Experimental verification of the theory of K

Experiment on surface tension isotherms of 0.5 mM sodium dodecyl sulfate (SDS)[44] at varying excess concentration of LiCl, NaCl and KCl showed significant differences due to the specific adsorptions of Li$^+$, Na$^+$, and K$^+$ counter-ions.
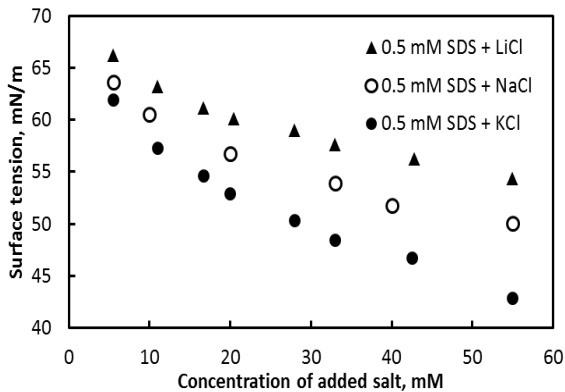
Figure 5. Surface tension isotherms of 0.5 mM SDS + added salts; The relative experimental error is ±0.2 mN/m.

The first experimental check will be the linearity of equation (35). We present hereafter the three adsorption isotherms in the scale of equation (35) and in CGS system. The concentration is converted in activity as well. The mean concentration is converted in mean activity.
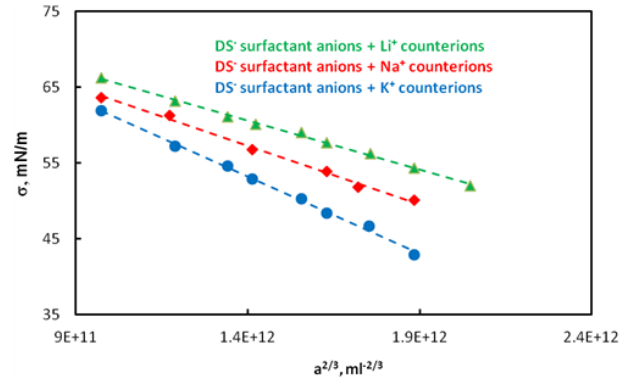
Figure 6. Surface tension isotherms of 0.5 mM SDS + added salts; The relative experimental error is ±0.2 mN/m.

One can see that **Figure 6** shows linear dependencies of the surface tension on the mean activity on 2/3 power ($a^{2/3}$). Therefore, equation (35) ($\sigma = \sigma_0 - 3RTKC^{2/3}$) is validated by the experiment. Moreover, one can calculate the equilibrium adsorption constants K for each of the cases from the slope (see equation (35)). Furthermore, equation (32) can be presented in the form:

$$lnK = lnK_0 - \frac{u_0}{2k_BT} \tag{48}$$

As far as the equilibrium adsorption constant K can be obtained experimentally by means of equa-

tion (35) and experimental surface tension isotherm, and u_0/k_BT can be calculated independently by means of equations (42) and (43) (see **Table 1**), lnK can be presented as a function of u_0/k_BT. **Figure 7** shows that lnK depends linearly on the specific adsorption energy of the counterions u_0/k_BT and the slope is close to ½, which is of validation of equation (48).
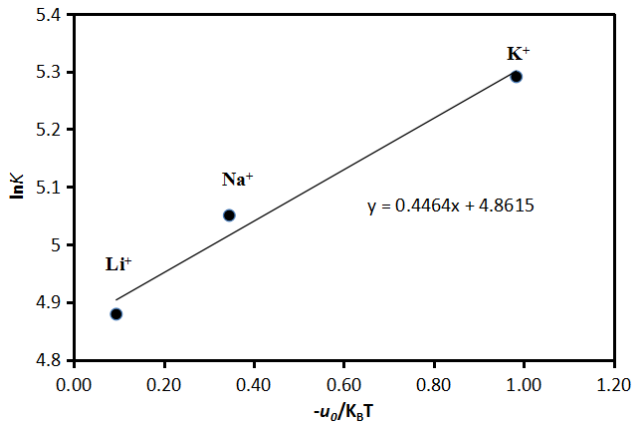

Figure 7. lnK as a function of $-u_0/k_BT$ for the cases SDS + LiCl, SDS + NaCl and SDS + KCl. In all of the cases the salt is added in great excess.
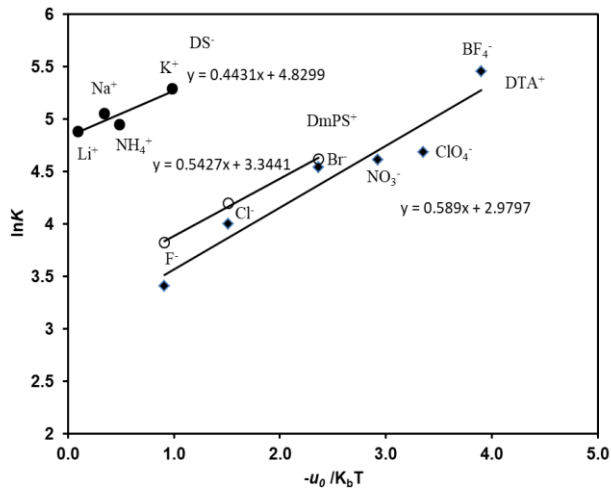
Figure 8. lnK as a function of $-u_0/k_BT$ for the cases (1) SDS + LiCl, SDS + NaCl, SDS + NH$_4$Cl, SDS + KCl; (2) DmPSCl + NaF, DmPSCl + NaCl, and DmPSCl + NaBr; and (3) DTAB + NaF, DTAB + NaCl, DTAB + NaNO$_3$, DTAB + NaClO$_4$, and DTABF$_4$[28].

Shown in **Figure 8** is presented lnK vs. $-u_0/k_BT$ for three types of surface active ions in presence of different counter-ions. In all of the cases, the slope of the line is close to ½, which validates well the presented above theory. The main question remaining is if this theory can predict the stability of dispersed systems.

3.2 Ion-specific effects on the stability of dispersed systems and relation to state of the adsorption layer[29,44]

3.2.1 Ion-specific effects on thin films and emulsions

The ion-specific effects on the state of the adsorbed surfactant layer influence the stability of foams and emulsions. This section is devoted to the investigation of the type of the surfactants counter-ion on the stability of the dispersed systems. It presents the experimental data of Ref.[29] and such one conducted in the present work.

Ref.[29] presents experimental data on the disjoining pressure of water films in air (foam films) stabilized by 1 mM solutions of hexadecyltrimethylammonium bromide (C$_{16}$H$_{33}$NMe$_3$Br) and 9 mM added salt (NaF, NaCl, NaBr).

The disjoining pressure, stabilizing the films, was measured on a thin film pressure balance by using the Mysels-Jones porous plate technique (see **Figure 9**).
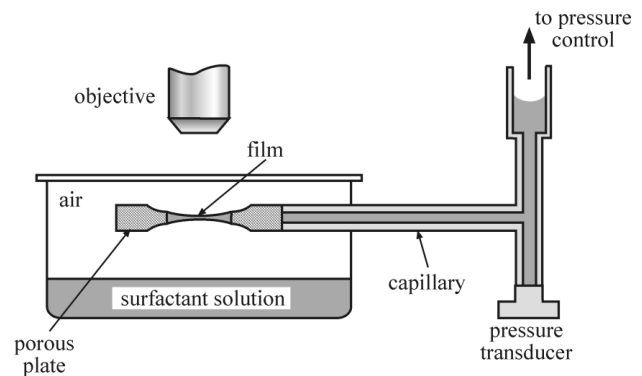

Figure 9. Schematic presentation of the porous plate cell.

The main question, which we raise, is how the type of the counter-ions affects the stability of foams and emulsions. We know from the previous sections that the counter-ions with a higher absolute value of the specific adsorption on air/water or oil/water interfaces are integrated onto the surfactant adsorption layer in larger degree and vice versa. Hence, at a higher level of counter-ion adsorption, the surface potential should be decreased more and vice versa. The theory of the electrostatic disjoining pressure has been developed by many authors, above all by Derjaguin and associates. Their results are summarized in the excellent book of Churaev *et al.*[45]. According to their theory (neglecting the ion specific effects), the electrostatic disjoining pres-

sure, Π_{el}, in a planar film of low surface potential or large thickness is given by the following expression:

$$\Pi_{el} = 64k_BTC_t\tanh^2\left(\frac{\Phi_{0S}}{4}\right)\exp(-\kappa h) = \Pi_0 exp(-\kappa h) \tag{49}$$

Where, C_t is total salt concentration, κ is the Debye constant, $\kappa = \sqrt{2F^2C_1/RT\varepsilon\varepsilon_0}$ and h is the thicknss of the thin liquid film. Since during the derivation of equation (49) in Ref.[45], no other assumptions about the surface potential were done, we decided that in order to account for the specific effects, it should be sufficient merely to replace Φ_{0s} with Φ_s by means of the following equation:

$$\Phi_S = \Phi_{0s} + \frac{u_0}{2k_BT} \tag{50}$$

Equation (49) suggests that the dependence of the experimental disjoining pressure Π on the thickness h should be close to linear in coordinating with $ln\,\Pi$ vs. h. **Figure 10** shows that indeed this is the case. Since the films are rather thick, one can disregard the contribution of the van der Waals disjoining pressure (direct numerical calculations confirmed this). This permits identifying Π with Π_{el} and using equation (49) for the calculation of Π, but with Φ_s replacing Φ_{s0}. The lines in **Figure 10** are almost parallel and obey the equation.

$$ln\Pi_{el} = ln\Pi_0 - \kappa h \tag{51}$$

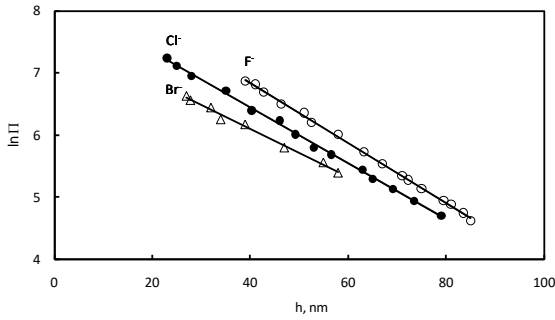The obtained intercepts $ln\Pi_0$ and slopes κ are shown in **Table 2.**

Figure 10. Plot of $ln\Pi$ vs. h for foam films stabilized with $C_{16}H_{33}NMe_3Br$ and NaX (X = F⁻, Cl⁻, Br⁻)**.**

Table 2. Intercepts, $ln\Pi_0$, and slopes, κ, of the lines in **Figure 10**.

Ion	F⁻	Cl⁻	Br⁻
$ln\Pi_0$ [Pa]	8.79	8.25	7.65
κ [nm⁻¹]	0.0485	0.0451	0.0386

The almost parallel, but shifted, lines suggest that the specific ion interactions (if any) are affected

mostly the surface potential Φ_s. By means of equation (49), we calculated the experimental values of Φ_s from the obtained data for Π_0 (see **Table 3**) and plotted in **Figure 11** the results as Φ_s vs. $-u_0/k_BT$. The relatively good linearity and close value of the experimental slope, 0.4, to the theoretical one, ½, (cf. Equation (50)) seem to confirm the role of the ion specific effect.
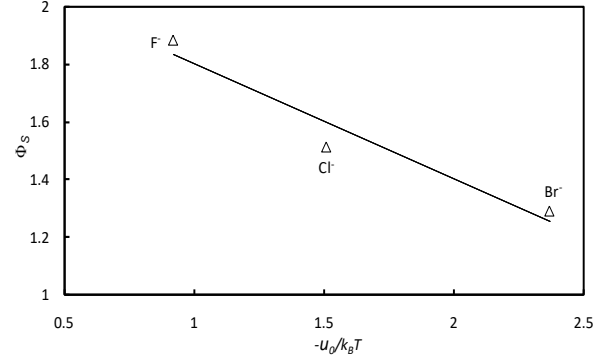
Figure 11. Combined surface potential Φ_s vs. $-u_0/k_BT$ for foam films stabilized with $C_{16}H_{33}NMe_3Br$ + NaX (X = F⁻, Cl⁻, Br⁻). The slope is –0.4**.**

The Hofmeister effect on the surface potential and the disjoining pressure, Π, is by no means negligible. To estimate it for films closer to reality, in **Figure 12,** we present the results (obtained in Ref.[26]) for the total disjoining pressure Π_{total} (including also the van der Waals contribution with Hamaker constant $A_H = 4\times10^{-20}$ J) of foam films with 0.5 mM of the halide counter-ions. The maxima of $\Pi(h)$ around $h = 5$ nm control the stability and the coalescence of the bubbles. The maximum is more than 4 times lower in the presence of only 0.5 mM Br than it would have been with the same electrolyte concentration if the ion specific effects were disregarded.
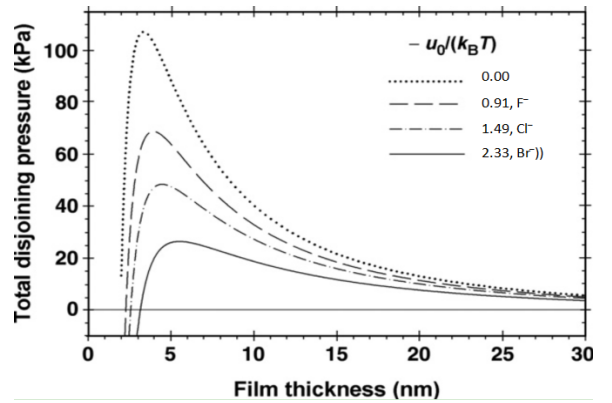
Figure 12. Total disjoining pressure Π_{total} calculated with Hamaker constant $A_H = 4\times10^{-20}$ J for 0.5 mM counterions F⁻, Cl⁻ and Br⁻ (from Ref.[26])**.**

Ref.[29] reports the emulsion stability measured by means of two types of techniques – Film Trapping Technique (FTT) and Centrifugation. They used the same surfactant ($C_{16}H_{33}NMe_3Br$) and salts (NaF, NaCl or NaBr). The concentrations of the surfactant and the added salts for FTT were the same as in the thin film studies described here above, but for the centrifugation, the emulsions with 1 mM salts were too unstable, so that the concentrations of the added salts were increased to 30 mM. Soybean oil, purified by passing it through a glass column filled with Silicagel 60 adsorbent, was used as oil phase.

The film trapping technique (FTT), developed in Refs.[46-49] is a useful method for determining the coalescence stability of single emulsion drops. The principle of the FTT is as following: A vertical capillary, partially filled with oil, is held at a small distance above the flat bottom of a glass vessel, **Figure 13**. The lower edge of the capillary is immersed in the working solution, which contains dispersed micron-size oil drops. The capillary is connected to a pressure control system, which allows one to vary and to measure precisely the difference, ΔP_A, between the air pressure in the capillary, P_A, and the atmospheric pressure, P_A^0. The pressure is measured by a pressure transducer connected to a personal computer. Upon the increase of P_A, the oil-water meniscus in the capillary moves downward against the substrate. When the distance between the oil-water meniscus and the glass substrate becomes smaller than the drop diameter, some of the drops remain entrapped in the formed glass-water-oil layer. The pressure P_A is increased until the coalescence of the entrapped oil drops with the upper oil phase is observed. The capillary pressure in the moment of drop coalescence, P_C^{CR}, represents the coalescence barrier and is called critical capillary pressure. It is related to ΔP_A in the moment of drop breakage and can be calculated from the equation:

$$P_C^{CR} = \Delta P_A - \Delta P_{OIL} - \rho g z \tag{52}$$

Where, ΔP_{OIL} is the pressure that jumps across the oil column in the capillary. It includes contributions from the hydrostatic pressure of the oil column and the capillary pressure of the air/oil meniscus. It is measured after filling the FTT capillary with oil, but before immersing the capillary into the water pool. In the hydrostatic term, z is the depth of the water (see **Figure 13**), ρ is the water mass density and g is gravity acceleration. The trapped oil drops and the coalescence process were observed from above with an optical microscope.
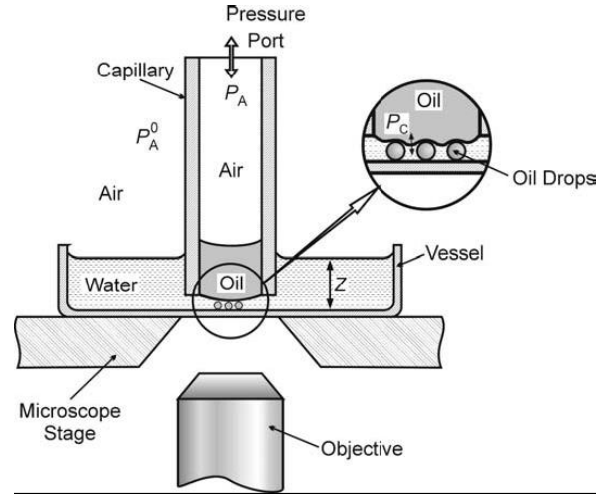

Figure 13. Scheme of the film trapping apparatus and of the droplets trapped between the oil-water and the substrate (see the magnification lens), from Ref.[49].

The test of the emulsion stability by means of centrifugation is described in details in Ref.[29]. Oil-in water emulsions were prepared by stirring for 4 min a mixture of 40 mL water phase and 10 mL soybean oil (20 vol. % SBO) with a rotor-stator homogenizer, Ultra Turrax T25 (Janke & Kunkel GmbH & Co, IKA-Labortechnik), operating at 13 500 rpm. The drop size d_{32} was determined by optical microscopy of specimens of the studied emulsions in transmitting light with a microscope. After 30 min storage, the fresh emulsions were transferred into several centrifugal tubes and centrifuged at 25 °C in 3K15 centrifuge. The emulsion stability is characterized by the critical osmotic pressure, P_{OSM}^{CR}, at which a continuous oil layer is released at the top of the emulsion cream in the centrifuge tube. P_{OSM}^{CR} is calculated from the experimental data by using the equation:

$$P_{OSM}^{CR} = \Delta \rho \, g_k (V^{OIL} - V^{REL})/A$$
$$= \Delta \rho g_k (H^{OIL} - H^{REL}) \tag{53}$$

Where, $\Delta \rho$ is the difference between the mass densities of the aqueous and the oil phases; g_k is the centrifugal acceleration ($g_k = L\omega^2$, where L is the distance between the axis of rotation and the center of the cream, ω is the angular velocity); V_{OIL} is the total volume of oil used for preparation of the

emulsion; V_{REL} is the volume of released oil at the end of centrifugation; and A is the cross-sectional area of the centrifuge test tube.

The results from both tests are presented in **Table 3** and **Figure 14**.

Table 3. Critical pressures and drop sizes of SBO-in-water emulsions, stabilized with 1 mM $C_{16}H_{33}NMe_3Br$ with added NaF, NaCl and NaBr

C_t [mM]	C_s [mM]	C_{el} [mM]	Electrolyte	d_{32} [m]	FTT, P_C^{CR} [Pa]	Centrifuge, P_{OSM}^{CR} [Pa]
10	1	9	NaF	25.2	360	-
10	1	9	NaCl	28.5	1100	-
10	1	9	NaBr	27.0	1320	-
31	1	30	NaF	20.7	-	360
31	1	30	NaCl	22.4	-	640
31	1	30	NaBr	21.5	-	917

The systems parameters and the measured values of the critical pressures P_C^{CR} and P_{OSM}^{CR} are tabulated in **Table 3** and plotted in **Figure 14** as P_C^{CR} (solid line) and P_{OSM}^{CR} (dashed line) vs. $-u_0/k_BT$. These critical pressures are proportional to Π and the higher their values are, the more stable the emulsions.

We do not dispose of enough information to carry out the same detailed analysis of these phenomena as we did with the electrostatic disjoining pressure. For example, we have no idea what the film thickness is; it is not quite clear whether a planar film forms or how much the disjoining pressure is affected by the curvature of the very small drops — these effects make problematic the calculation of the electrostatic disjoining pressure by means of equation (49). Still, some qualitative conclusions are possible. The linear dependence of P_C^{CR} and P_{OSM}^{CR} on $-u_0/k_BT$ confirms the presence of specific effects. However, instead of decreasing with the increase of $-u_0/k_BT$ (as the electrostatic disjoining pressure does), the critical pressures are increasing. Therefore, the electrostatic disjoining pressure Π_{all} is not the repulsive pressure to be overcome in order for the coalescence to occur. But then, what is the reason for the ion specific effect, demonstrated in **Figure 14**? It is not possible to answer with certitude this question without detailed studies of the phenomena accompanying the coalescence process. Nevertheless, we dare suggesting a hypothesis. The role of the specific effect of the counter-ions is twofold. On one side, it decreases the height of the

maxima of the disjoining pressure (see **Figure 15**), thus, making easier for the thin film to avoid the electrostatic repulsive pressure and from thin to thinner (metastable) Newton black film, where another, short range repulsive disjoining pressure (most probably steric or osmotic) might be operative.
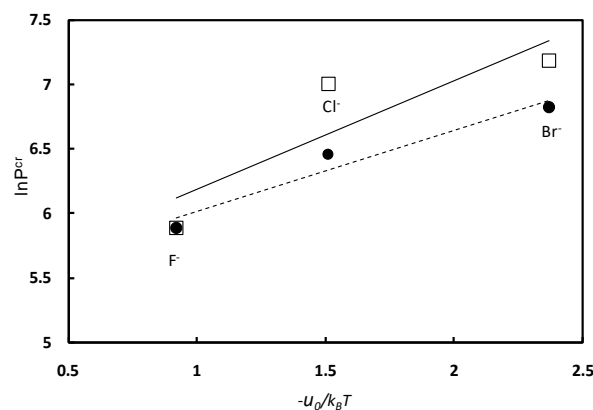

Figure 14. Critical pressures P_C^{CR} (by FTT, solid line) and P_{OSM}^{CR} (by centrifugation, dashed line) vs. $-u_0/k_BT$ of oil-in-water emulsions stabilized by $C_{16}H_{33}NMe_3Br$ + NaX (X = F$^-$, Cl$^-$, Br$^-$). ($\square$) P_{OSM}^{CR} of oil-in-water emulsion films stabilized by 10^{-3} M $C_{16}H_{33}NMe_3Br$ + 9×10^{-3} M NaX (X = F$^-$, Cl$^-$, Br$^-$) obtained by FTT (slope = 0.85); ($\bullet$) P_C^{CR} of oil-in-water emulsion films stabilized by 10^{-3} M $C_{16}H_{33}NMe_3Br$ + 3×10^{-2} M NaX (X = F$^-$, Cl$^-$, Br$^-$) obtained by centrifuge (slope = 0.63).
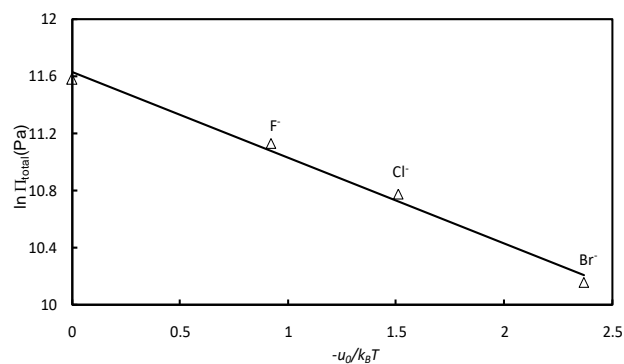

Figure 15. Total disjoining pressure Π_{total} in the maxima in **Figure 12** vs. $-u_0/k_BT$. This is in fact the coalescence barrier, according to DLVO theory.

It must be overcome for the thin film to rupture. On the other side, no matter what the nature of this disjoining pressure is, it must increase with the surfactant adsorption, Γ. However, unlike the electrostatic disjoining pressure, the surfactant adsorption, Γ, increases (for a given bulk surfactant concentration) with $-u_0/k_BT$. This brings us to the second role of the ion specific effects – it is to increase the short range repulsive pressure created by the surfactant, thus stabilizing the thin film. This ex-

plains why the slopes of the lines in **Figure 14** are positive. They should have been negative if only the electrostatic disjoining pressure Π_{el} were stabilizing the film. To support this opinion in **Figure 15**, we have plotted the maxima of Π_{total} from **Figure 12** (which are in fact the coalescence barriers), vs. $-u_0/k_BT$ indeed, the slope is negative. This means that the short range repulsive pressure involved in the stability of the emulsion drops is not directly related to ion specific effects. The theoretical and experimental verification of this hypothesis is feasible, but it is time consuming and beyond the scope of this paper.

3.2.2 Ion-specific effects on foams

We have established that the stability of the emulsions increases upon enhancing the specific adsorption energy of the counter-ions. This tendency was not expected.

For this reason, we were challenged to investigate this scientific "intrigue" deeper. We have chosen another system – foam stabilized by sodium dodecyl sulfate (SDS) and LiCl, NaCl and KCl as salts, which were meant to be added in an amount significantly exceeding this one of the surfactant.

We clearly showed hereafter that the electrostatic repulsion between the bubbles, which is controlled by the added counter-ions, is only one of the factors contributing to foam stabilization. The counter-ions strongly affect the level of surfactant adsorption as well. The latter appears to be decisive for the stabilization of the foam and the foam films. We show as well some new effects originating from the counter-ions, which have practical significance.

Sodium dodecyl sulfate (SDS) with molecular weight $M_w = 288.38$ Da, an anionic surfactant, lithium chloride (LiCl) with molecular weight $M_w = 42.29$ Da, sodium chloride (NaCl) with molecular weight $M_w = 58.44$ Da, and potassium chloride (KCl) with molecular weight $M_w = 74.55$ Da were purchased from Sigma Aldrich. The surfactant was purified by threefold recrystallization in ethanol.

SDS salt mixture solutions were prepared as follows. Initially, using SDS, 0.5 mM aqueous solution was prepared. Then, LiCl, NaCl and KCl, were added, thus forming salt solutions with concentrations in the range of 2.5 mM, to 50 mM. As far as the foaming ability of every surfactant solution is expressed in both the initial foam volume upon the very generation of foam and the lifetime of the latter, we chose to work with the ratio between the two values, called foam production[50]. The foam was produced by means of the Bartsch method expressed in energetical tenfold shaking of Bartsch column containing 50 ml of the surfactant solution. Each experiment was repeated at least 3 times for statistical certainty, the averaged initial foam volume and lifetimes were determined. Thus, the foam production for every particular case was calculated. The basic results are presented in **Figure 16**.

One can see that the foam production increases linearly upon the increase of the specific energy of counter-ions adsorption in the range of 2.5 mM to 11 mM added salt (see **Figure 16A**). Moreover, this linear dependence is violated by K^+ counter-ion at concentrations of added salt above 11 mM (see **Figure 16B**, **16C**, **16D**). The foam production decreases significantly abruptly at 25 mM KCl. This low value of the foam production remains at a larger concentration of KCl. They correspond to both low initial foam volume and fast foam decay.

This abnormal effect of KCl on the foam production is worthy of further investigation. Possible way for such an investigation to explore the properties of single foam films with the same contents as these ones was shown in **Figure 16**. Moreover, it is curious to know if the critical concentration at which the K^+ ion acts as defoamer depends on the method of foam generation.

The experimental data presented in **Figure 16A** are in line with the experimental data reported in Ref.[29]. The stability of the dispersed system increases upon the increase of the absolute value of the specific adsorption energy of the counter-ions on the air/water interface. Most possibly, this is due to the increased level of the surfactant adsorption when more counter-ions are integrated in the surfactant adsorption layer. However, to investigate this effect on deeper level further investigations are needed.
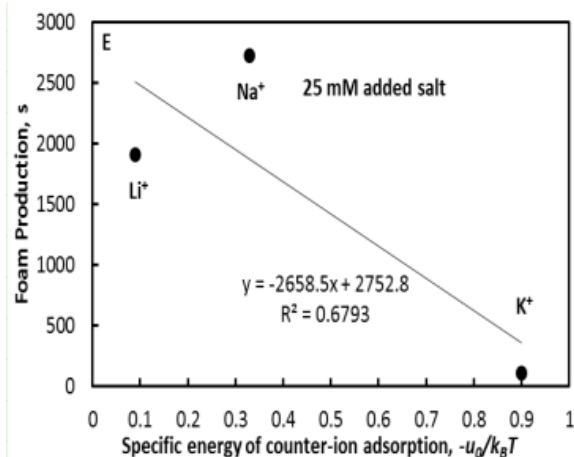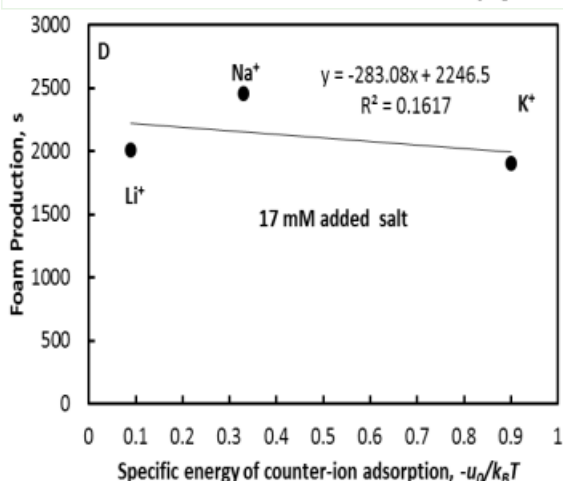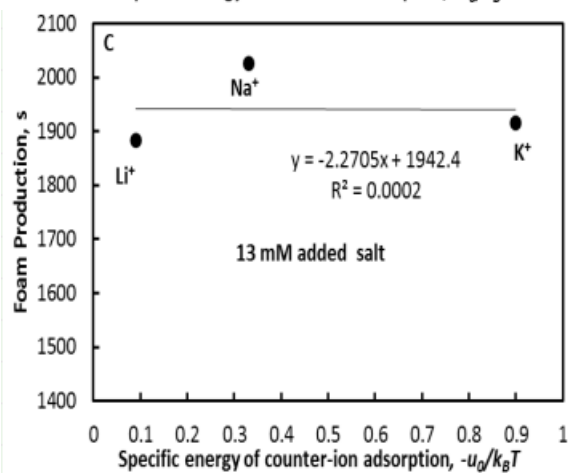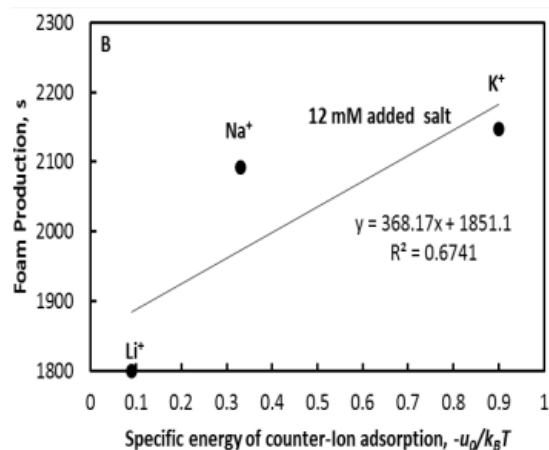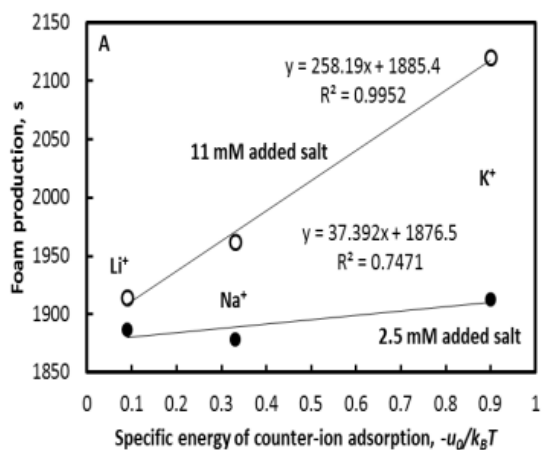
Figure 16. Foam production versus specific energy of counter-ion adsorption at concentrations of added salt in the range of 2.5 mM – 25 mM.

4. Conclusions

The ion-specific effects on the adsorption of ionic surfactants are known effect. There is a large body of literature on this topic, but it is spread out in many papers and books at present. It is known as well that the counter-ions affect the state of the adsorbed layers, which influences the stability of the colloidal dispersions, but the effect is not studied completely. This manuscript gathers together a detailed description of the theory on the ion-specific effects on the adsorption of ionic surfactants in its first approximation (Davies adsorption isotherm) and some initial experimental studies of the Hofmeister effect on the stability of foams and emulsions. Thus, we show the nature of the effect of the counter-ions on the state of the equilibrated surfactant adsorption layer, while we stress that their effect on the stability of colloidal dispersions can be non-equilibrated, thus giving an origin of new tendencies. It was shown that the counter-ions can have a dual effect on the stability of foams and emulsions, depending on the concentration of the added salt. We call for further investigations on this interesting effect, which might be used for controlling the stability of foams and emulsions for industrial needs.

Conflict of interest

No conflict of interest was reported by the author.

65

Acknowledgements

References

1 Lewith S. The behaviour of the proteins in the blood serum in the presence of salts. Archiv Fuer Experimentelle Pathologie und Pharmakologie 1887; XXIX: 1–16.

2 Hofmeister F. About regularities in the protein precipitating effects of salts and the relation of these effects with the physiological behaviour of salts. Archiv Fuer Experimentelle Pathologie und Pharmakologie 1887; XXIV: 247–60.

3 Hofmeister F. About the water withdrawing effect of the salts. Archiv Fuer Experimentelle Pathologie und Pharmakologie 1888; XXV: 1–30.

4 Limbeck Rv. About the diuretic effect of salts. Archiv Fuer Experimentelle Pathologie und Pharmakologie 1888; XXV: 69–86.

5 Hofmeister F. Investigations about the swelling process. Archiv Fuer Experimentelle Pathologie und Pharmakologie 1890; XVII: 395–413.

6 Hofmeister F. The contribution of dissolved components to swelling processes. Archiv Fuer Experimentelle Pathologie und Pharmakologie 1991; XXVIII: 210–38.

7 Muenzer E. The general effect of salts. Archiv Fuer experimentelle Pathologie und Pharmakologie 1898; XLI: 74–96.

8 Kunz W. Specific ion effects in colloidal and biological systems. Current Opinion in Colloid & Interface Science 2010; 15: 34–9.

9 Kunz W, Lo Nostro P, Ninham BW. The present state of affairs with Hofmeister effects. Current Opinion in Colloid & Interface Science 2004; 9: 1–18.

10 Ninham BW, Yaminsky V. Ion binding and ion specificity: The Hofmeister effect and Onsager and Lifshitz theories. Langmuir 1997; 13: 2097–108.

11 Bostrom M, Williams DRM, Ninham BW. Specific ion effects: Why DLVO theory fails for biology and colloid systems. Physical Review Letters 2001; 87.

12 Bostroem M, Williams DRM, Ninham BW. Surface tension of electrolytes: Specific ion effects explained by dispersion forces. Langmuir 2001; 17: 4475–8.

13 Bostrom M, Kunz W, Ninham BW. Hofmeister effects in surface tension of aqueous electrolyte solution. Langmuir 2005; 21: 2619–23.

14 Moreira LA, Bostrom M, Ninham BW, *et al.* Hofmeister effects: Why protein charge, pH titration and protein precipitation depend on the choice of background salt solution. Colloids and Surfaces A: Physicochemical and Engineering Aspects 2006; 282: 457–63.

15 Bostroem M, Ninham BW. Contributions from dispersion and born self-free energies to the solvation energies of salt solutions. The Journal of Physical Chemistry B 2004; 108: 12593–5.

16 Tavares FW, Bratko D, Blanch HW, *et al.* Ion-specific effects in the colloid-colloid or protein-protein potential of mean force: Role of salt-macroion van der Waals interactions. The Journal of Physical Chemistry B 2004; 108: 9228–35.

17 Warszynski P, Lunkenheimer K, Czichocki G. Effect of counterions on the adsorption of ionic surfactants at fluid-fluid interfaces. Langmuir 2002; 18: 2506–14.

18 Para G, Jarek E, Warszynski P. The Hofmeister series effect in adsorption of cationic surfactants - theoretical description and experimental results. Advances in Colloid and Interface Science 2006; 122: 39–55.

19 Para G, Jarek E, Warszynski P. The surface tension of aqueous solutions of cetyltrimethylammonium cationic surfactants in presence of bromide and chloride counterions. Colloids and Surfaces A: Physicochemical and Engineering Aspects 2005; 261: 65–73.

20 Li HH, Imai Y, Yamanaka M, *et al*. Specific counter-ion effect on the adsorbed film of cationic surfactant mixtures at the air/water interface. Journal of Colloid and Interface Science 2011; 359: 189–93.

21 Shimamoto K, Onohara A, Takumi H, W *et al*. Miscibility and distribution of counter-ions of imidazolium ionic liquid mixtures at the air/water surface. Langmuir 2009; 25: 9954–9.

22 Hayami Y, Ichikawa H, Someya A, *et al.* Thermodynamic study on the adsorption and micelle formation of long chain alkyltrimethylammonium chlorides. Colloid and Polymer Science 1998; 276: 595–600.

23 Davies JT. Adsorption of long-chain ions I. Proceedings of the Royal Society of London. Series A 1958; 245: 417–28.

24 Davies JT, Rideal EK. Interfacial Phenomena, 2nd ed. New York: Academic Press; 1963.

25 Borwankar RP, Wasan DT. Equilibrium and dynamics of adsorption of surfactants at fluid-fluid interfaces. Chemical Engineering Science 1988; 43: 1323–37.

26 Ivanov IB, Marinova KG, Danov KD, *et al*. Role of the counter-ions on the adsorption of ionic surfactants. Advances in Colloid and Interface Science 2007; 134-135: 105–24.

27 Ivanov IB, Ananthapadmanabhan KP, Lips A. Adsorption and structure of the adsorbed layer of ionic surfactants. Advances in Colloid and Interface Science 2006; 123-126: 189–212.

28 Slavchov RI, Karakashev SI, Ivanov IB. Ionic surfactants and ion-specific effects: Adsorption, micellization, thin liquid films. In: Romsted LS (editor). Surfactant science and technology: Retrospects and prospects. New York: Taylor & Francis Group; 2014. p. 593.

29 Ivanov IB, Slavchov RI, Basheva ES, *et al.* Hof-

meister effect on micellization, thin films and emulsion stability. Advances in Colloid and Interface Science 2011; 168: 93–104.

30   Robinson RA, Stokes RH. Electrolyte Solutions. 2nd ed. London: Butterworths Scientific Publications; 1959. p. 560.

31   Lucassen-Reynders EH. Surface equation of state for ionized surfactants. The Journal of Physical Chemistry 1966; 70: 1777–85.

32   Davies JT. Study of foam stabilizers using a new (\"viscous-traction\") surface viscometer. Proceedings of the Second International Congress of Surface Activity 1957: 220–4.

33   Lu JR, Marrocco A, Su T, et al. Adsorption of dodecyl sulfate surfactants with monovalent metal counter-ions at the air-water interface studied by neutron reflection and surface tension. Journal of Colloid and Interface Science 1993; 158: 303–16.

34   Israelachvili JN. Intermolecular and surface forces. New York: Academic Press; 1985.

35   Jones G, Ray WA. The surface tension of solutions of electrolytes as a function of the concentration. III. Sodium chloride. Journal of the American Chemical Society 1941; 63: 3262–3.

36   Collins KD. Charge density-dependent strength of hydration and biological structure. Biophysical Journal 1997; 72: 65–76.

37   Marcus Y. Effect of ions on the structure of water: Structure making and breaking. Chemical Reviews 2009; 109: 1346–70.

38   Marcus Y. Ion properties. New York: Marcel Dekker; 1997.

39   Marcus Y. Thermodynamics of ion hydration and its interpretation in terms of a common model. Pure and Applied Chemistry 1987; 59: 1093–101.

40   Kunz W, Belloni L, Bernard O, et al. Osmotic coefficients and surface tensions of aqueous electrolyte solutions: Role of dispersion forces. The Journal of Physical Chemistry B 2004; 108: 2398–404.

41   Nikolskij BP. Handbook of the Chemist (In Russian). Moscow: Khimia; 1966.

42   Dietrich B, Kintzinger JP, Lehn JM, et al. Stability, molecular-dynamics in solution, and X-Ray structure of the ammonium cryptate $[NH_4^+ \subset 2.2.2]PF_6^-$. Journal of Physical Chemistry 1987; 91: 6600–6.

43   Lide DR. CRC Handbook of chemistry and physics. 83rd ed. New York, London: CRC Press; 2002. p. 2664.

44   Sett S, Karakashev SI, Smoukov SK, et al. Ion-specific effects in foams. Advances in Colloid and Interface Science 2015; 225: 98–113.

45   Churaev NV, Derjagiun BV, Muller VM. Surface Forces. New York: Springer; 1987. p. 440.

46   Ivanov IB, Hadjiiski A, Denkov ND, et al. Energy of adhesion of human T cells to adsorption layers of monoclonal antibodies measured by a film trapping technique. Biophysical Journal 1998; 75: 545–56.

47   Hadjiiski A, Dimova R, Denkov ND, et al. Film trapping technique - Precise method for three-phase contact angle determination of solid and fluid particles of micrometer size. Langmuir 1996; 12: 6665–75.

48   Hadjiiski A, Tcholakova S, Ivanov IB, et al. Gentle film trapping technique with application to drop entry measurements. Langmuir 2002; 18: 127–38.

49   Tcholakova S, Denkov ND, Ivanov IB, et al. Coalescence in beta-lactoglobulin-stabilized emulsions: Effects of protein adsorption and drop size. Langmuir 2002; 18: 8960–71.

50   Karakashev SI, Georgiev P, Balashev K. Foam production — ratio between foaminess and rate of foam decay. Journal of Colloid and Interface Science 2012; 379: 144–7.

67